Information-Theoretic Lifetime Maximization for IoBNT-Enabled Sensing

Koca, Caglar; Ozger, Mustafa; Cetinkaya, Oktay; Akan, Ozgur B.

Published in:
IEEE Transactions on Molecular, Biological, and Multi-Scale Communications

DOI (link to publication from Publisher):
10.1109/TMBMC.2025.3562353

Publication date:
2025

Document Version
Accepted author manuscript, peer reviewed version

Information-theoretic Lifetime Maximization for IoBNT-enabled Sensing

Caglar Koca, *Student Member, IEEE,* Mustafa Ozger, Oktay Cetinkaya, *Senior Member, IEEE,* and Ozgur B. Akan, *Fellow, IEEE*

***Abstract*—Internet of Things (IoT) translates the physical world into a cyber form using wireless sensors. However, these sensors often lack longevity due to their energy-constrained batteries. This limitation is particularly critical for the Internet of Bio-Nano Things (IoBNT), in which sensors usually operate within an organism with minimum opportunities for replenishment. Thus, adopting energy-efficient strategies is vital to maximize the lifetime of such sensors and ensure the reliable execution of associated applications. To address this, this letter proposes an event-driven, time-adaptive transmission scheme based on the Kullback-Leibler (KL) distance. Specifically, the KL distance is used to measure the worth of transmitting the current sensor reading, enabling the sensor to decide whether to transmit in that sampling period, thereby saving energy and extending its lifetime. Furthermore, we identify the operational regions for sensors, namely *safe*, *unsafe*, and *action*, depending on application-specific parameters. The design and implementation of the required circuitry are also discussed, considering the unique constraints of the IoBNT. Performance evaluation validates that the KL distance improves sensor lifetime with an acceptable information loss.**

***Index Terms*—Shannon Entropy, Information Priority, IoT, IoBNT, Lifetime Maximization.**

I. Introduction

Internet of Things (IoT) helps us monitor and control our surroundings over the Internet using smart devices with sensing and actuation capabilities. Thanks to its numerous benefits, IoT has been widely applied across various domains, ranging from embedded systems [1] and distributed sensing [2] to Smart Grids [3] and drone/UAV networking [4].

Internet of Bio-Nano Things (IoBNT), an extension of IoT, seeks to bring Internet connectivity to tissues, cells, and even bacteria [5]–[7]. This ambitious vision inevitably imposes two essential requirements: *miniaturization* and *biocompatibility*. Miniaturization further constrains already limited energy resources, such as batteries and energy harvesters [8], while biocompatibility adds additional design complexities, particularly concerning power provisioning [9]. As a result, IoBNT not only inherits the shortcomings of the IoT but also introduces its unique challenges, making energy efficiency of paramount importance for sensor longevity [10]–[12].

Despite the immense efforts, lifetime maximization is still an open research issue in both IoT and IoBNT domains [13]. Previously, more capable sensor nodes, e.g., sinks, were designated as local data-storing proxies [14]. For mobile sinks, optimal data collection schedules and efficient channel coding strategies were proposed to enhance communication throughput besides energy efficiency [15], [16]. Information-theoretic approaches to increase network lifetime were also studied as in [17], where the authors utilized *Differential Kullback-Leibler (KL) distance* to detect outliers within the clusters of a network with minimum energy used. To elaborate, the KL distance is a natural and intuitive metric to assign a value to a measurement [18], [19]. This makes it well-suited for assessing the changes in sensor readings, a critical factor in minimizing unnecessary data transmissions, which is an inherently energy-intensive task for sensors. However, since the IoBNT circuitry has to be both small and consume minimum energy to prevent tissue damage [20], continuous calculation of KL distance is impractical for this domain. Hence, successful approximations of KL distance using low power and small circuitry are essential for the IoBNT sensors.

In this letter, we use the KL distance to measure the information value of transmitting consecutive sensor readings to preserve energy. Based on this metric, we calculate application-specific thresholds before deployment that satisfy a quality of service (QoS) target. In this way, the sensor decides whether to transmit its last reading with a simple comparison. If this comparison indicates that the KL distance between the readings is below the aforementioned threshold, the current reading is not sent to the sink. The sensors diligently report dramatic changes and provide some data in the absence of large deviations, informing the users of both the events and the general characteristics of the parameter of interest. Hence, the sensors operate in an *event-driven* and *time-adaptive* manner. This proposed transmission scheme does not rely on complex circuitry following the unique IoBNT requirements.

Our contributions in this letter can be itemized as below:

- Developing a new data transmission scheme that reconciliates event-driven and time-adaptive approaches for sensor lifetime maximization,
- Proposing an implementation framework for our scheme, particularly motivated for IoBNT applications.

The remainder of this paper is organized as follows. Sec. II introduces the system model, followed by the proposed transmission scheme in Sec. III. Then, the additional hardware

C. Koca and O. B. Akan are with the Center for neXt-generation Communications (CXC), Department of Electrical and Electronics Engineering, Koç University, Istanbul 34450, Turkey (e-mail: {cagkoca, akan}@ku.edu.tr).

M. Ozger is with the Department of Electronic Systems, Aalborg University, Copenhagen, Denmark (e-mail: mozger@es.aau.dk).

O. Cetinkaya is with the School of Engineering, Newcastle University, Newcastle upon Tyne NE1 7RU, UK. (e-mail: oktay.cetinkaya@newcastle.ac.uk).

O. B. Akan is also with the Internet of Everything (IoE) Group, Electrical Engineering Division, Department of Engineering, University of Cambridge, Cambridge CB3 0FA, UK (email: oba21@cam.ac.uk).

This work was supported in part by the AXA Research Fund (AXA Chair for Internet of Everything at Koç University).

requirements for implementing this scheme are discussed in Sec. IV. Finally, simulation results are presented in Sec. V before concluding the paper in Sec. VI.

II. System Model

A. System Elements

Our system model considers a generic IoBNT network consisting of multiple sensors and sinks. Each sensor is dedicated to observing a particular variable, denoted as the parameter of interest (PoI). PoI values randomly fluctuate in time, which can either be insignificant or include some jumps. For instance, we consider the changes in the heart rate while the person is sitting as small, whereas sudden jumps may occur when an event happens, e.g., when the person stands up. We can obtain the PoI profile, which includes but is not limited to, periodicities, positive or negative feedbacks and asymptotic behaviors, via long-term observation and statistical analysis.

Sensors have uncertainties, ϵ, which usually depend on the measured value, i.e., $\epsilon(s)$. The uncertainty profiles of the sensors are usually provided in their datasheet. For simplicity, we use the commonly used assumption that the sensor is perfectly accurate, except for a constant additive Gaussian noise, $\mathcal{N}(0, \epsilon)$ [21], [22].

Following the measurements, the sinks collect the associated values and send them to the cloud over the Internet. To preserve energy, before sending their readings, the sensors first analyze the information value of transmitting the current reading using the KL distance. We assume that the sink–sensor connection is reliable.

B. Operational Regions

We define three regions of operation: safe, unsafe, and action regions, as shown in Fig. 1. The region boundaries are application-specific, i.e., they depend on the PoI volatility, sensor parameters, and safety constraints. In the *safe region*, the PoI values do not deviate much from the last reading. Even if there are sudden jumps, the probability of the system sliding into the action region from the safe region is negligible by definition.

Action region is where the PoI reaches values that necessitate an immediate action. In the action region, we cannot assume that PoI values do not deviate much from the last reading. Note that, the action region may be influenced by positive feedback, ensuring large and continuous changes in the PoI value.

Finally, we define the *unsafe region* through exclusion. Any value of PoI that is not in the safe region and does not require immediate action is in the unsafe region. Here, the sensor readings are still predictable, but there is a high risk of the system sliding into the action region. Thus, by definition of the unsafe region, preserving energy might reduce the chance of an early action in the unsafe region. As a result, in the unsafe region, we abandon our scheme entirely and revert to the frequency-driven transmission.

We can use a continuous health monitoring application, measuring and transmitting temperature values for illustrative purposes. Generally, body temperature is between 36.1 °C and 37.2 °C. Thus, measurements within this range fall in the safe region. Temperature values between 35.5 °C – 36.1 °C and between 37.2 °C – 38.0 °C are in the unsafe region, as the former points to initial stages of possible hypothermia and the latter emergence of a fever. If the measured values are lower than 35.5 °C or higher than 38.0 °C, we need to take immediate action. Note that, sensor nodes operating at different parts of the body need to be calibrated differently. For example, sensor nodes operating at the extremities should have different borders for the operational regions than the nodes operating around the brain.

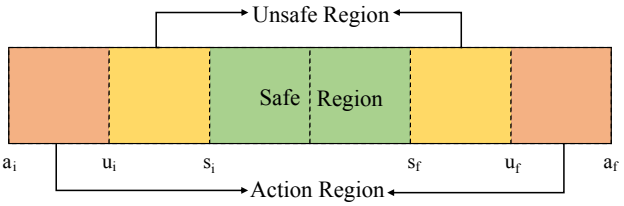

Fig. 1: The operational regions of the sensor node.

III. Transmission Scheme

Assume that a sensor node with a sampling period of ΔT reads a value of α at time T, i.e., $s(T) = \alpha$ and relays it to the sink. If the next sensor reading is β, i.e., $s(T + \Delta T) = \beta$, we denote the information value of transmitting this reading as $V(s(T + \Delta T) = \beta | s(T) = \alpha)$, which we shorten by $V(\beta|\alpha)$.

Note that, as long as the sink has access to a statistical profile of PoI, it can *guess* the next sensor reading. More specifically, the sink knows that the current sensor reading, $\hat{s}$, has a probability density function (PDF) $f_{\hat{s}}(\hat{s}|\alpha)$, centered around α. Recalling our discussion from Sec. II-A, sensor readings also do not reflect the exact value of the PoI. In other words, the exact value of the PoI, $\tilde{s}$, has a PDF of $f_{\tilde{s}}(\tilde{s}|\beta)$. We illustrate $f_{\hat{s}}(\hat{s}|\alpha)$ and $f_{\tilde{s}}(\tilde{s}|\beta)$ in Fig. 2.

Since the sensor node knows α, β, and the time since the transmission of α, the node can calculate $V(\beta|\alpha)$, the informa-

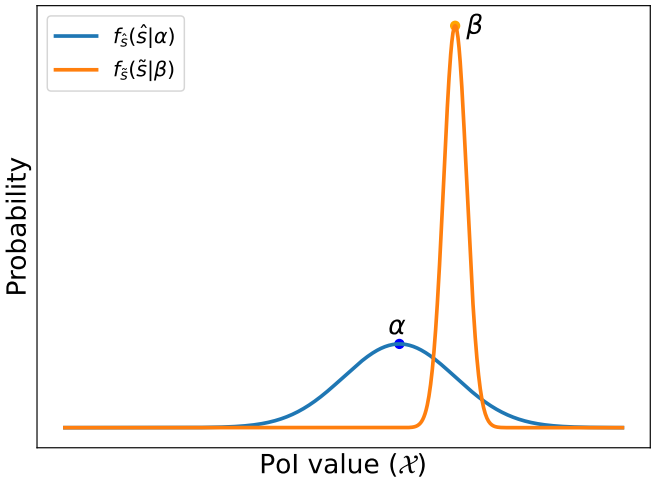

Fig. 2: Illustration of $f_{\hat{s}}(\hat{s}|\alpha)$ and $f_{\tilde{s}}(\tilde{s}|\beta)$. Note that, with realistic simulation parameters, $f_{\tilde{s}}(\tilde{s}|\beta)$ would be much narrower.

tion gained by the sink, if the node transmits $s(T+\Delta T)=\beta$. Qualitatively, $V(\beta|\alpha)$ is the information difference between what the sink can guess about $s(T+\Delta T)$ from $s(T)=\alpha$ and how confident the sensor is of $s(T+\Delta T)=\beta$. We calculate $V(\beta|\alpha)$ with the expression:

$$V(\beta|\alpha)=D_{KL}(f_{\hat{s}}(\hat{s}|\alpha)||f_{\tilde{s}}(\tilde{s}\beta)), \tag{1}$$

where D_{KL} stands for the KL distance. Qualitatively, (1) states the unpredictability of $s(T+\Delta T)=\beta)$ when $s(T)=\alpha$ is provided.

The time evolution of the PoI is application–specific. Hence, to evaluate (1), we first need to find $f_{\tilde{s}}(\tilde{s}|\beta)$ and $f_{\hat{s}}(\hat{s}|\alpha)$ using the sensor's and PoI's statistical profile, respectively. However, if such a sensor profile does not exist, without loss of generality, we use the additive Gaussian noise sensor model [21], [22], as we describe in Sec. II-A, i.e.:

$$f_{\tilde{s}}(\tilde{s}|\beta)=\frac{1}{\sqrt{2\pi\epsilon^2}}\exp\left(-\frac{(\beta-\tilde{s})^2}{2\epsilon^2}\right). \tag{2}$$

Similarly, if there is no statistical information on the PoI, we assume that sensor readings follow a one-dimensional (1D) Brownian Motion (BM) model for the safe and unsafe regions, where sensor readings are predictable, i.e., large transitions in readings are not expected. Hence, within the safe and unsafe regions, the sink knows that $\hat{s}=s(T+\Delta T)$ follows the PDF:

$$f_{\hat{s}}(\hat{s}|\alpha)=\frac{1}{\sqrt{4\pi D\Delta T}}\exp\left(-\frac{(\alpha-\hat{s})^2}{4D\Delta T}\right), \tag{3}$$

where D is the PoI volatility, analogous to the mass diffusivity of BM. Here, we assume that the variation after a single sampling period dominates the variation due to the sensor uncertainty, i.e., $2D\Delta T\gg\epsilon^2$. Using (3), we express (1) as:

$$V(\beta|\alpha)=\log\frac{\epsilon}{\sqrt{2D\Delta T}}+\frac{2D\Delta T+(\beta-\alpha)^2}{2\epsilon^2}-\frac{1}{2}. \tag{4}$$

Note that, $V(\beta|\alpha)$ is only a function of $|\beta-\alpha|$.

To preserve energy, the node decides to remain silent if $V(\beta|\alpha)<k$, where k is the QoS threshold for the loss of information. However, to compute $V(\beta|\alpha)$ before each transmission, the sensor requires dedicated hardware and computational energy. Thus, instead of computing $V(\beta|\alpha)$ before each transmission, we check whether the difference satisfies $V(\beta|\alpha)<k$, by comparing it with the maximum, i.e., threshold difference, i.e.:

$$|\beta-\alpha|_{th}=\max|\beta-\alpha|:V(\beta|\alpha)<k, \tag{5}$$
$$=|\beta-\alpha|:V(\beta|\alpha)=k. \tag{6}$$

Note that $k\to 0$ makes the system frequency-driven as $|\beta-\alpha|\to 0$. Similarly, $k\to\infty$ turns the system into an event-driven one as $|\beta-\alpha|\to\infty$. In other words, for $k\to 0$, all measurements are transmitted while for $k\to\infty$, no measurement within the safe region is transmitted. Therefore, the users can adjust k to reach an application-specific optimum.

The sensor compares the difference between the last transmitted reading with the current one with a pre-calculated value satisfying (6). The comparison serves to decide whether to proceed with the transmission, with the pre-calculated $|\beta-\alpha|_{th}$ being:

$$|\beta-\alpha|_{th}=\left|\left(k+\frac{1}{2}-\log\left(\frac{\epsilon}{\sqrt{2D\Delta T}}\right)\right)2\epsilon^2-2D\Delta T\right|^{\frac{1}{2}}. \tag{7}$$

Hence, as long as $|\beta-\alpha|$ is smaller than $|\beta-\alpha|_{th}$, which is a function of k, ϵ, D, and ΔT, the system remains silent, i.e., preserve energy. However, even this process might require extra hardware. To avoid using large and complex circuitry, we suggest bitwise comparison. Let b_m be the most significant bit of $|\beta-\alpha|_{th}$, i.e.:

$$b_m=\lceil\log_2(|\beta-\alpha|_{th})\rceil. \tag{8}$$

If $|\beta-\alpha|<2^{b_m}$, we know that $|\beta-\alpha|<|\beta-\alpha|_{th}$. As a result, the sensor decides not to transmit its last reading. Since this approach requires checking only the most significant bit of $|\beta-\alpha|$, we denote it as *binary Kullback–Leibler distance* (KLb).

The sensor may remain silent if the upcoming readings are also close to the last transmitted value. However, the ability of the sink to successfully guess $s(T+i\Delta T)$ deteriorates, where i is the consequent silences. For $i>1$, $f_{\hat{s}}(\hat{s}|\alpha)$ becomes $f^i_{\hat{s}}(\hat{s}|\alpha)$, i.e.:

$$f^i_{\hat{s}}(\hat{s})=\frac{1}{\sqrt{4\pi Di\Delta T}}\exp\left(-\frac{(\alpha-\hat{s})^2}{4Di\Delta T}\right). \tag{9}$$

Similarly, we can calculate $V^i(\beta|\alpha)$, $|\beta-\alpha|^i_{th}$ and b^i_m by substituting $\Delta t\leftarrow i\Delta t$ to (4), (7) and (8), respectively.

Evident from (7), $|\beta-\alpha|^i_{th}$ decreases rapidly as i increases. To compensate for the diminishing silent region, we calculate b^i_m with (8) by substituting $|\beta-\alpha|^i_{th}$ for $|\beta-\alpha|_{th}$.

The silent region after each silent period becomes smaller, and it eventually vanishes when $|\beta-\alpha|^i_{th}=0$. Extrapolating further, we see that regardless of how close the last sensor reading to the last transmitted value is, after a certain number of silent periods, n_{KL}, $V(\beta|\alpha)$ cannot be smaller than k.

Theorem 1. *The sensor node cannot stay silent any longer than n_{KL} sampling periods, n_{KL} being:*

$$n_{KL}=\left\lfloor\frac{\mathcal{W}_{-1}(-\ln(2)2^{-2k-1})\epsilon^2}{-\ln(2)2D\Delta T}\right\rfloor, \tag{10}$$

where $\mathcal{W}_{-1}$ is the -1^{th} branch of the multi-valued Lambert-W function, which is defined as:

$$z=x\exp x\iff x=\mathcal{W}(z). \tag{11}$$

Suppose the sensor remains silent longer than n_f periods. In that case, the sink may consider a malfunction and decide to take preemptive action against a possible interruption in the observed system.

Corollary 1. *The sink assumes the node malfunctions if it stays silent longer than n_f periods, n_f being:*

$$n_f=\left\lfloor\frac{-\ln(1-l)}{\lambda\Delta T}\right\rfloor. \tag{12}$$

where λ is the failure rate, and l is an application-specific QoS parameter.

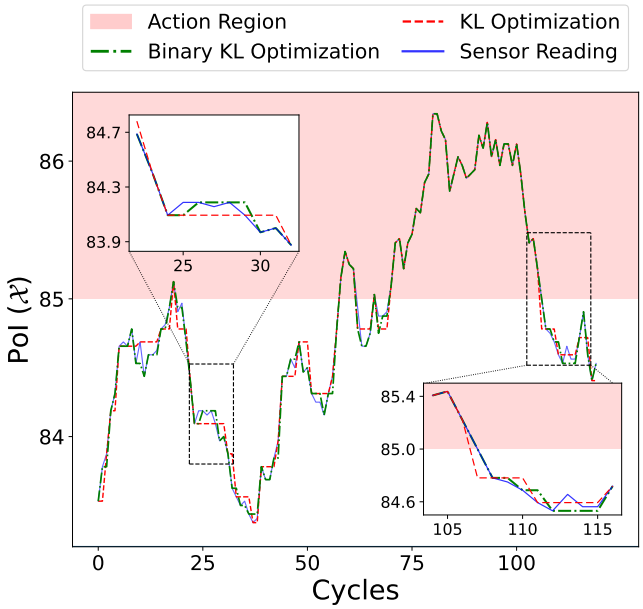

Fig. 3: Illustration of unoptimized sensor reading with the KL optimized and binary KL optimized transmissions.

We provide the proofs for Theorem 1 and Corollary 1 in Appendix A and Appendix B, respectively.

Combining (10) and (12), the silent period limit becomes:

$$n_{lim} = \min\left(n_{KL}, n_f\right). \tag{13}$$

IV. Implementation

As mentioned previously, constantly comparing the KL distance of readings requires computational power and extra components. Hence, especially for IoBNT applications, we need an efficient circuit to approximate the KL distance, as it is hard to implement bio-compatible, nano-sized, complex circuits [10].

For a fast and efficient decision-making process, we first compute the value matrix. Assuming (2) and (3) holds, i.e., V only depends on the $|\beta - \alpha|$, for a sensor with an m-bit output, (13) we construct an n_{lim} by m matrix, with each entry calculated as:

$$V_{uv} = D_{KL}(f^v_{\hat{s}}(\hat{s}|\alpha)||f_{\tilde{s}}(\tilde{s}|\beta), \tag{14}$$

where u is the most significant bit of $|\beta-\alpha|$, i.e., $u = \lceil \log(\beta-\alpha) \rceil$, and v is the consecutive silent periods. Qualitatively, the V matrix carries the values of sending transmissions after $v-1$ silent periods, if u is the most significant bit of $|\beta - \alpha|$.

Using the V matrix and the allowed k value, we construct the K matrix that compares V_{ij} with k, i.e.:

$$K_{ij} = \begin{cases} 1, & \text{for } V_{ij} < k, \\ 0, & \text{for } V_{ij} \geq k. \end{cases} \tag{15}$$

To decide whether to proceed with the next transmission, we can use a simple logic circuitry consisting of a register (to hold the previous transmission), a subtractor, a counter (to hold the silent periods), and a priority encoder. Two registers are also required to mark the boundaries of the safe region. If the safe region is constant, we can carve its boundaries onto a Read-Only Memory (ROM) to save energy. Furthermore, we can avoid any overhead in the sleep cost by employing a register with no refresh need. Hence, our only energy overhead would be computational power, which may be neglected compared to transmission power.

In cases where (2) and (3) do not hold, the implementation becomes application-specific, which falls outside the scope of this letter. However, as long as the PoI and sensor profiles exist, we can find low-order approximations for V_{uv} and design our circuit accordingly.

V. Performance Evaluation

To assess the performance of our proposed transmission scheme, we present the results of Monte Carlo simulations. The simulations were conducted using Python version 3.11.3, with pseudorandom numbers generated via the built-in function in NumPy version 1.24.3. We assume the observed variable mostly obeys the 1D BM model within the safe region. However, we also include random events, with a much higher amplitude than that of the random walk steps. We use the exponential failure model for the component. Table I provides the simulation parameters.

The sensor is capable of making 12-bit measurements, excluding the sign bit, thus allowing us to measure the values from -127.96875 to 127.96875. Since we have chosen $[-85, 85]$ as our safe region, the node transmits all measurements outside this region.

In Fig. 3, we demonstrate the closeness of the sensor data to the data transmitted to the sink. By visual inspection, we see that after KL or binary KL optimizations, the PoI value remains constant for some periods, implying that the sensor did not transmit in that period. Note that sensor readings, KL and binary KL optimizations are superimposed in the action region, as we drop our transmission scheme outside the safe region.

The relationship between the silent period ratio and tolerable KL distance, k, is given in Fig. 4. As expected, as k increases, the node transmits fewer PoI values, reaching 93% for $k = 4000$. Note that the node does not remain silent for $s < -85$ and $s > 85$, which mark the boundaries of the safe region.

TABLE I: Simulation parameters.

Parameter	*Value*	*Unit*	*Symbol*
Bits	12		m
Most significant bit	7		b_m
Sensor volatility	10^{-4}	$\mathcal{X}^2 s^{-1}$	D
Sampling period	10^3	ms	ΔT
Sensor variance	$1/32$	$\mathcal{X}$	ϵ
Expected sensor life	10^{10}	ms	$1/\lambda$
Safe regions	$[-85, 85]$	$\mathcal{X}$	$\mathcal{S}$
Event probability	5×10^{-5}		q_p
Event amplitude	50		q_a
Tolerable KL distance	25		k
Tolerable sensor breakdown probability	0.001		l

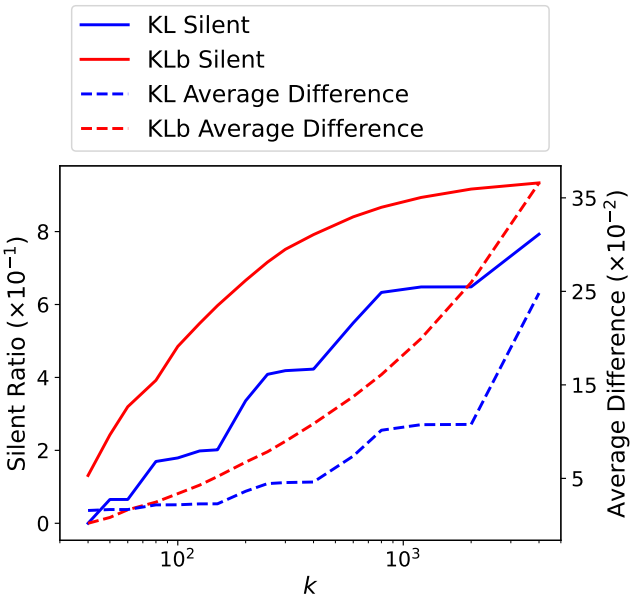

Fig. 4: Silent ratio and the average difference between the PoI values sent to the sink and the sensor measured vs. k, the tolerable KL distance.

In other words, the 7% transmissions include cases where we abandon our scheme and return to frequency-driven reporting. However, even when the node remains silent for more than 90% of the sampling periods, the average difference between the measured at the sensor and estimated at the sink is less than 0.4. For comparison, the total range of the sensor is ~ 256.

Examining Fig. 4, we see that the simulation results of the binary KL optimization display sudden jumps. These jumps, arising from (8), indicate the points where the increase in k causes the most significant bit to change. As expected, KLb optimization is less potent than KL optimization. For regular IoT applications, KL optimization might be better since transmission costs are usually much higher than computational costs. However, for IoBNT applications, the nodes might have limited computational power, so binary KL optimization might be the only feasible option.

VI. Conclusions

This letter proposes an event-driven and time-adaptive transmission scheme based on the KL distance between sensor readings in an IoBNT-enabled WSN. By reconciling the event-driven and frequency-driven transmission schemes, our approach allows energy-restricted WSNs, such as IoBNT applications, to seamlessly monitor more extended periods with limited loss of information. We also put forward the binary KL optimization, a novel approach designed to take the specific constraints of the IoBNT vision. We characterize the operational regions of sensors and the overall energy efficiency of the operation. The design procedure of the required circuit to perform the operations of the proposed scheme was also provided. Performance evaluation validates that the KL distance could achieve energy-efficient data transmission with an acceptable and predetermined information loss while achieving the maximum lifetime.

References

[1] D. Balsamo *et al.*, "A Control Flow for Transiently Powered Energy Harvesting Sensor Systems," *IEEE Sensors Journal*, vol. 20, no. 18, pp. 10 687–10 695, 2020.
[2] O. Cetinkaya *et al.*, "Distributed Sensing with Low-Cost Mobile Sensors Toward a Sustainable IoT," *IEEE Internet of Things Magazine*, vol. 4, no. 3, pp. 96–102, 2021.
[3] E. B. Pehlivanoglu *et al.*, "Harvesting-Throughput Trade-off for Wireless-Powered Smart Grid IoT Applications: An Experimental Study," in *2018 IEEE International Conference on Communications (ICC)*, 2018, pp. 1–6.
[4] T. Long *et al.*, "Energy Neutral Internet of Drones," *IEEE Communications Magazine*, vol. 56, no. 1, pp. 22–28, 2018.
[5] I. F. Akyildiz *et al.*, "The internet of bio-nano things," *IEEE Communications Magazine*, vol. 53, no. 3, pp. 32–40, 2015.
[6] S. Angerbauer *et al.*, "Novel nano-scale computing unit for the iobnt: Concept and practical considerations," *IEEE Transactions on Molecular, Biological, and Multi-Scale Communications*, 2024.
[7] G. Rampioni *et al.*, "Gene-expressing liposomes as synthetic cells for molecular communication studies," *Frontiers in bioengineering and biotechnology*, vol. 7, p. 1, 2019.
[8] D. Jing, L. Lin, and A. W. Eckford, "Energy allocation for multi-user cooperative molecular communication systems in the internet of bio-nano things," *IEEE Internet of Things Journal*, 2024.
[9] M. Civas *et al.*, "Graphene and related materials for the internet of bio-nano things," *APL Materials*, vol. 11, no. 8, 2023.
[10] S. Balasubramaniam *et al.*, "Multi-hop conjugation based bacteria nanonetworks," *IEEE Transactions on Nanobioscience*, vol. 12, no. 1, pp. 47–59, 2013.
[11] M. Kuscu and B. D. Unluturk, "Internet of bio-nano things: A review of applications, enabling technologies and key challenges," *arXiv preprint arXiv:2112.09249*, 2021.
[12] O. B. Akan *et al.*, "Internet of hybrid energy harvesting things," *IEEE Internet of Things Journal*, vol. 5, no. 2, pp. 736–746, 2018.
[13] M. Ozger, E. B. Pehlivanoglu, and O. B. Akan, "Energy-efficient transmission range and duration for cognitive radio sensor networks," *IEEE Transactions on Cognitive Communications and Networking*, 2021.
[14] T. P. Raptis, A. Passarella, and M. Conti, "Maximizing industrial iot network lifetime under latency constraints through edge data distribution," in *2018 IEEE Industrial Cyber-Physical Systems (ICPS)*. IEEE, 2018, pp. 708–713.
[15] M. A. Habib *et al.*, "Lifetime maximization of sensor networks through optimal data collection scheduling of mobile sink," *IEEE Access*, vol. 8, pp. 163 878–163 893, 2020.
[16] C. Bai, M. S. Leeson, and M. D. Higgins, "Minimum energy channel codes for molecular communications," *Electronics Letters*, vol. 50, no. 23, pp. 1669–1671, Nov. 2014.
[17] G. Li and Y. Wang, "Differential kullback-leibler divergence based anomaly detection scheme in sensor networks," in *2012 IEEE 12th International Conference on Computer and Information Technology*. IEEE, 2012, pp. 966–970.
[18] P. Padhy *et al.*, "A utility-based adaptive sensing and multihop communication protocol for wireless sensor networks," *ACM Transactions on Sensor Networks (TOSN)*, vol. 6, no. 3, pp. 1–39, 2010.
[19] J. Zhang, Z. Li, and S. Tang, "Value of information aware opportunistic duty cycling in solar harvesting sensor networks," *IEEE Transactions on Industrial Informatics*, vol. 12, no. 1, pp. 348–360, 2015.
[20] I. F. Akyildiz *et al.*, "Microbiome-gut-brain axis as a biomolecular communication network for the internet of bio-nanothings," *IEEE Access*, vol. 7, pp. 136 161–136 175, 2019.
[21] N. Cao *et al.*, "Sensor selection for target tracking in wireless sensor networks with uncertainty," *IEEE Transactions on Signal Processing*, vol. 64, no. 20, pp. 5191–5204, 2016.
[22] B. Xia and C. Mi, "A fault-tolerant voltage measurement method for series connected battery packs," *Journal of Power Sources*, vol. 308, pp. 83–96, 2016.